



## **EFFECS OF INPUT DIRECTION OF GROUND MOTION AND COLUMN OVERDESIGN FACTOR ON SEISMIC RESPONSE OF 3D STEEL MOMENT FRAMES**

I. Chan<sup>(1)</sup>, Y. Koetaka<sup>(2)</sup> and K. Suita<sup>(3)</sup>

<sup>(1)</sup> Graduate Student, Dept. of Architecture and Architectural Engineering, Kyoto Univ. M. Eng., chan.hong.45r@st-kyoto-u.ac.jp

<sup>(2)</sup> Assoc. Prof., Dept. of Architecture and Architectural Engineering, Kyoto Univ. Dr. Eng., koetaka@archi.kyoto-u.ac.jp

<sup>(3)</sup> Prof., Dept. of Architecture and Architectural Engineering, Kyoto Univ. Dr. Eng., suita@archi.kyoto-u.ac.jp

### **Abstract**

Steel moment frames should be designed to ensure sufficient energy absorption capacity by achieving an entire beam-hinging collapse mechanism under severe earthquakes. Therefore, the column overdesign factor is stipulated in seismic design codes of several countries. Since both orthogonal plane frames are designed as moment resisting frames in Japan, square tube columns are often used for steel building structures. Therefore bi-axial bending moment acts on the columns under bi-direction ground motion. On that occasion, the apparent full plastic moment of the square tube column, which is projected on the direction parallel to the frame plane, under bi-axial bending moment is smaller than the full plastic moment under a uni-axial bending moment. Considering the effect of bi-direction ground motions on the steel moment frames, the specified column overdesign factor is 1.5 or more in Japanese seismic design code.

A lot of numerical studies on the required column overdesign factor have been conducted in order to ensure beam-hinging responses under uni-direction ground motion. On the other hand, there are few researches about the required column overdesign factor of steel moment resisting frames under bi-direction ground motions.

This paper describes seismic response by 3D analysis of steel moment frames, and presents seismic demand for the column overdesign factor to keep the damage of square tube columns below the specified limit of plastic deformation. The major parameters are column overdesign factor of beam-column connections, number of stories, the planar shape of frames, input direction of earthquake.

In order to investigate 3D behavior of frames and correlation between plastic deformation of columns and column over design factor, apparent column overdesign factor, which is defined as the ratio of full plastic moment of the column(s) to the full plastic moment of the beam(s) projected in the input direction of the ground motion, is introduced. As a result of earthquake response analysis, cumulative plastic deformation of columns decreases and cumulative plastic deformation of beams increases, when apparent column overdesign factor becomes larger. The profile of maximum value of cumulative plastic deformation of columns to apparent column overdesign factor are nearly identical regardless of number of stories, floor plan, and input direction of ground motion.

As an index to evaluate the damage of columns, the plastic deformation capacity of square tube columns depending on local buckling is adopted for different rank of width-thickness ratio, and the damage level of columns is defined as the value obtained by dividing cumulative plastic deformation by plastic deformation capacity. From the relationship between apparent column overdesign factor and the damage level of columns, the required column overdesign factor to keep the damage level below the specified value is proposed.

For example, the required apparent column overdesign factor for frames with  $D_s$  value of 1/3, under level 2 ground motion, to keep the cumulative plastic deformation below the performance limit is obtained as 1.40 for square tube columns of FA rank width-thickness ratio, and 1.60 for FB rank, 1.83 for FC rank, respectively.

*Keywords: 3D Steel Moment Frame; Multi-spring Model; Column Overdesign Factor; Input Direction of Ground Motion*



## 1. Introduction

Steel moment frames should be designed to ensure sufficient energy absorption capacity by achieving an entire beam-hinging collapse mechanism under severe earthquakes. Therefore, the column overdesign factor (*COF*) is stipulated in seismic design codes of several countries.

For example, wide flange columns are often used for steel building structures in United States [1]. Only one of the orthogonal plane frames is designed as moment resisting frames, because the beam-to-column connections around the weak axis of the columns are designed as pin-joint. Hence, considering the moment resisting frames under uni-direction ground motion, the specified *COF* is 1.0 or more in AISC seismic design code [2]. On the other hand, square tube columns are often used in Japan, and both orthogonal plane frames are designed as moment resisting frames. Therefore bi-axial bending moment acts on the columns under bi-direction ground motion. On this occasion, the apparent full plastic moment of the square tube column, which is projected on the direction parallel to the frame plane, under bi-axial bending moment is smaller than the full plastic moment under a uni-axial bending moment. Considering the effect of bi-direction ground motions on the steel moment frames, the specified *COF* is 1.5 or more in Japanese seismic design code [3].

A lot of numerical studies on the required *COF* have been conducted in order to ensure beam-hinging responses under uni-direction ground motions [4-16]. On the other hand, there are few researches about the required *COF* of steel moment frame under bi-direction ground motions [17-21]. In comparison to the required *COF* under uni-direction ground motions, it has been shown that a much larger *COF* is needed under bi-direction ground motions. Focus on the 3D analysis model used in Ref. [17-19], 3D frames were simplified to fishbone-shaped model, which can not show the damage distribution of each structural member. Since *COF* was not taken to be a parameter in Ref. [20-21], in which 3D frame model was used, the required *COF* was not proposed.

Therefore, this paper describes seismic response of steel moment frames, e.g. damage of each member, by 3D dynamic analysis, and presents seismic demand for the *COF* to keep the damage of square tube columns below the specified limit of plastic deformation. The major parameters are *COF* of beam-column connections, number of stories, floor plan, input direction of earthquake.

## 2. Method of Analysis

### 2.1 Fundamental assumptions

- 1) 3D model is used in this paper. Each structural member is taken to be a simplified model with bar element.
- 2) Connections between beams and columns are considered rigid. Panels are ignored.
- 3) Nodal points have 6 degrees of freedom, 3 translational and 3 rotational axes.
- 4) Weight and mass are concentrated on nodal points.
- 5) Member models consist of an elastic component and 2 multi-spring components (MS component in the following) as shown in Fig.1.
- 6) The length of elastic component is the same length as the original member. Axial, bending, shear and torsion deformations are considered in the elastic component.
- 7) Only axial and bending deformations are considered in MS components. MS components consist of several elasto-plastic springs, in which only axial deformation is considered. MS components are assumed to have no length within the member model, but are assigned a virtual length for calculating spring stiffness.
- 8) Geometrical nonlinearity is not considered.

### 2.2 Coordinate systems

In coordinate systems, there is a global coordinate system where the 3D model is based, as well as separate member coordinate systems for each member model. The global coordinate system is fixed on the ground surface. Each member coordinate system has its origin at the *i*-end and moves with the member, its z-axis connects the *i* and *j*-ends, the strong-axis at the *i*-end is considered the x-axis, while the weak-axis is the y-axis.

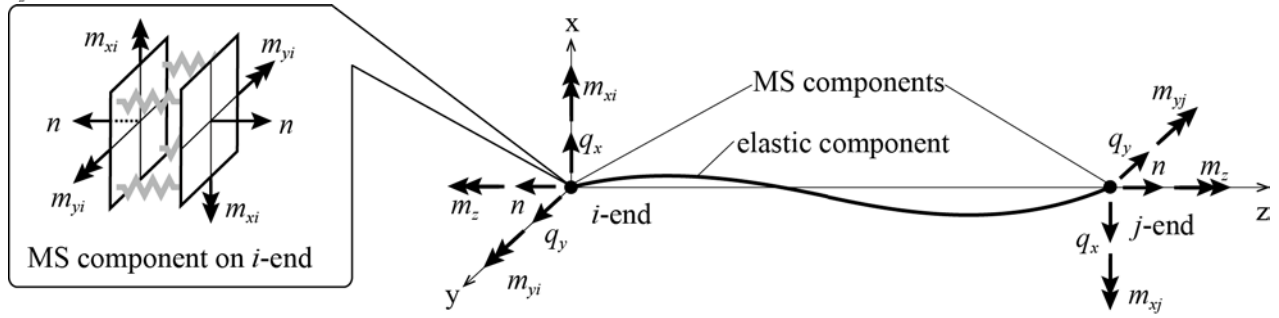


Fig.1 – Member model

### 2.3 Stiffness matrix of the member model

As shown in Fig.1, we consider at both ends of the member model an axial force  $n$ , shear forces  $q_x$  and  $q_y$ , bending moments  $m_x$  and  $m_y$  and a torsion moment  $m_z$ . From assumption 4), the incremental force vector is given by Eq. (1). Here,  $\Delta$  denotes a small increment, the subscripts  $i$  and  $j$  refer to origin and end points respectively.

$$\{\Delta \mathbf{p}\} = \left\{ \Delta n \quad \Delta m_{xi} \quad \Delta m_{xj} \quad \Delta m_{yi} \quad \Delta m_{yj} \quad \Delta m_z \right\}^T \quad (1)$$

The incremental deformation vector corresponding to Eq. (1) is given by Eq. (2).

$$\{\Delta \mathbf{d}\} = \left\{ \Delta d \quad \Delta \theta_{xi} \quad \Delta \theta_{xj} \quad \Delta \theta_{yi} \quad \Delta \theta_{yj} \quad \Delta \theta_z \right\}^T \quad (2)$$

From assumption {6} and {7}, the incremental deformation vector of the elastic component  $\{\Delta \mathbf{d}_e\}$  is given by Eq. (3), the incremental deformation vector of the MS components at the  $i$  and  $j$ -ends  $\{\Delta \mathbf{d}_i\}$ ,  $\{\Delta \mathbf{d}_j\}$  are given by Eq. (4) and Eq. (5) respectively.

$$\{\Delta \mathbf{d}_e\} = \left\{ \Delta d^e \quad \Delta \theta_{xi}^e \quad \Delta \theta_{xj}^e \quad \Delta \theta_{yi}^e \quad \Delta \theta_{yj}^e \quad \Delta \theta_z \right\}^T \quad (3)$$

$$\{\Delta \mathbf{d}_i\} = \left\{ \Delta d_i^{ms} \quad \Delta \theta_{xi}^{ms} \quad 0 \quad \Delta \theta_{yi}^{ms} \quad 0 \quad 0 \right\}^T \quad (4)$$

$$\{\Delta \mathbf{d}_j\} = \left\{ \Delta d_j^{ms} \quad 0 \quad \Delta \theta_{xj}^{ms} \quad 0 \quad \Delta \theta_{yj}^{ms} \quad 0 \right\}^T \quad (5)$$

The constitutive equation of each member is written as Eq. (6) by using the stiffness matrix  $[\mathbf{k}]$ .

$$\{\Delta \mathbf{d}\} = \{\Delta \mathbf{d}_i\} + \{\Delta \mathbf{d}_e\} + \{\Delta \mathbf{d}_j\} = [\mathbf{k}]^{-1} \{\Delta \mathbf{p}\} \quad (6)$$

$[\mathbf{k}]^{-1}$  in Eq. (6) is found by adding the tangential flexibility matrices of the elastic and MS components, which are the inverse matrices of their respective tangential stiffness matrices. The tangential stiffness equations of the MS components are as Eq. (7) and Eq. (8). In the force-deformation relationship of the spring component the tensile side is taken to be positive.  $k_s$  denotes the stiffness of the  $s$ -th spring,  $x_s$ ,  $y_s$  denote its coordinates in the member coordinate system.

$$\begin{Bmatrix} \Delta n \\ \Delta m_{xi} \\ \Delta m_{yi} \end{Bmatrix} = \begin{bmatrix} \Sigma k_s & -\Sigma k_s y_s & \Sigma k_s x_s \\ & \Sigma k_s y_s^2 & -\Sigma k_s x_s y_s \\ Sym. & & \Sigma k_s x_s^2 \end{bmatrix} \begin{Bmatrix} \Delta d_i^{ms} \\ \Delta \theta_{xi}^{ms} \\ \Delta \theta_{yi}^{ms} \end{Bmatrix} \quad (7)$$



$$\begin{Bmatrix} \Delta n \\ \Delta m_{xj} \\ \Delta m_{yj} \end{Bmatrix} = \begin{bmatrix} \Sigma k_s & \Sigma k_s y_s & -\Sigma k_s x_s \\ & \Sigma k_s y_s^2 & -\Sigma k_s x_s y_s \\ Sym. & & \Sigma k_s x_s^2 \end{bmatrix} \begin{Bmatrix} \Delta d_j^{ms} \\ \Delta \theta_{xj}^{ms} \\ \Delta \theta_{yj}^{ms} \end{Bmatrix} \quad (8)$$

Hence, the tangential flexibility matrices of the MS components are Eq. (9) and Eq. (10).

$$\begin{bmatrix} {}_i c_z & {}_i c_y & {}_i c_x \\ & {}_i c_{yy} & {}_i c_{xy} \\ Sym. & & {}_i c_{xx} \end{bmatrix} = \begin{bmatrix} \Sigma k_s & -\Sigma k_s y_s & \Sigma k_s x_s \\ & \Sigma k_s y_s^2 & -\Sigma k_s x_s y_s \\ Sym. & & \Sigma k_s x_s^2 \end{bmatrix}^{-1} \quad (9)$$

$$\begin{bmatrix} {}_j c_z & {}_j c_y & {}_j c_x \\ & {}_j c_{yy} & {}_j c_{xy} \\ Sym. & & {}_j c_{xx} \end{bmatrix} = \begin{bmatrix} \Sigma k_s & \Sigma k_s y_s & -\Sigma k_s x_s \\ & \Sigma k_s y_s^2 & -\Sigma k_s x_s y_s \\ Sym. & & \Sigma k_s x_s^2 \end{bmatrix}^{-1} \quad (10)$$

The tangential flexibility matrix of the elastic component  $[c_e]$  is given by Eq. (11). Here,  $A_z$  is the cross-sectional area,  $A_{sx}$  and  $A_{sy}$  the shear cross-sectional areas of the x and y-axes,  $I_x$  and  $I_y$  the second moment around the x and y-axes,  $I_z$  the torsion constant,  $E$  the Young modulus, and  $G$  the shear modulus. Shear deformation of the elastic component is considered by the terms containing  $G$  represent shear flexibility in  ${}_e c_z$ ,  ${}_e c_{yy}$ ,  ${}_e c_y$ ,  ${}_e c_{xx}$ ,  ${}_e c_x$  and  ${}_e c_{zz}$  according to Timoshenko's beam theory. The initial flexibility matrix of the member model, which can be got by summing the initial flexibility matrices of the elastic and MS components, differs from that of the actual member. This is because of the assumption 7) about the length of the MS components in the member model. The terms containing  $k_s'$ , where  $k_s'$  is the initial stiffness of the  $s$ -th spring, are to account for the difference.

$$[c_e] = \begin{bmatrix} {}_e c_z & 0 & 0 & 0 & 0 & 0 \\ & {}_e c_{yy} & {}_e c_y & 0 & 0 & 0 \\ & & {}_e c_{yy} & 0 & 0 & 0 \\ & & & {}_e c_{xx} & {}_e c_x & 0 \\ & & & & {}_e c_{xx} & 0 \\ Sym. & & & & & {}_e c_{zz} \end{bmatrix} \quad (11a)$$

$${}_e c_z = \frac{l}{EA_z} - \frac{2}{\Sigma k_s'}, \quad {}_e c_{yy} = \frac{l}{3EI_x} - \frac{1}{\Sigma k_s' y_s^2} + \frac{1}{GA_{sy} l}, \quad {}_e c_y = -\frac{l}{6EI_x} + \frac{1}{GA_{sy} l} \quad (11b)$$

$${}_e c_{xx} = \frac{l}{3EI_y} - \frac{1}{\Sigma k_s' x_s^2} + \frac{1}{GA_{sx} l}, \quad {}_e c_x = -\frac{l}{6EI_y} + \frac{1}{GA_{sx} l}, \quad {}_e c_{zz} = \frac{l}{GI_z} \quad (11c)$$

The tangential stiffness matrix of a member is given as Eq. (12).



$$[\mathbf{k}] = \begin{bmatrix} e C_z + i C_z + j C_z & i C_y & j C_y & i C_x & j C_x & 0 \\ & e C_{yy} + i C_{yy} & e C_y & i C_{xy} & 0 & 0 \\ & & e C_{yy} + j C_{yy} & 0 & j C_{xy} & 0 \\ & & & e C_{xx} + i C_{xx} & e C_x & 0 \\ & & & & e C_{xx} + j C_{xx} & 0 \\ & Sym. & & & & e C_{zz} \end{bmatrix}^{-1} \quad (12)$$

## 2.4 Coordinate Transformation matrices and the global stiffness matrix

From assumption 3), the coordinate system has 6 degrees of freedom, hence in the global coordinate system, the incremental force vector  $\{\Delta \mathbf{P}\}$  and incremental displacement vector  $\{\Delta \mathbf{D}\}$  of member model, as given by Eq. (13) and Eq. (14), have 12 dimensions.

$$\{\Delta \mathbf{P}\} = \left\{ \Delta P_{Xi} \quad \Delta P_{Yi} \quad \Delta P_{Zi} \quad \Delta M_{Xi} \quad \Delta M_{Yi} \quad \Delta M_{Zi} \quad \Delta P_{Xj} \quad \Delta P_{Yj} \quad \Delta P_{Zj} \quad \Delta M_{Xj} \quad \Delta M_{Yj} \quad \Delta M_{Zj} \right\}^T \quad (13)$$

$$\{\Delta \mathbf{D}\} = \left\{ \Delta D_{Xi} \quad \Delta D_{Yi} \quad \Delta D_{Zi} \quad \Delta \Theta_{Xi} \quad \Delta \Theta_{Yi} \quad \Delta \Theta_{Zi} \quad \Delta D_{Xj} \quad \Delta D_{Yj} \quad \Delta D_{Zj} \quad \Delta \Theta_{Xj} \quad \Delta \Theta_{Yj} \quad \Delta \Theta_{Zj} \right\}^T \quad (14)$$

The relations between  $\{\Delta \mathbf{P}\}$  and  $\{\Delta \mathbf{p}\}$ ,  $\{\Delta \mathbf{D}\}$  and  $\{\Delta \mathbf{d}\}$  at the  $n$ -th step are Eq. (15) and Eq. (16), where  $[\mathbf{S}]$  is a 12x6 matrix, and  $[\mathbf{T}_n]$  the  $n$ -th step coordinate transformation matrix.

$$\{\Delta \mathbf{P}_n\} = [\mathbf{T}_n][\mathbf{S}]\{\Delta \mathbf{p}_n\} \quad (15)$$

$$\{\Delta \mathbf{D}_n\} = [\mathbf{T}_n][\mathbf{S}]\{\Delta \mathbf{d}_n\} \quad (16)$$

Since the member coordinate system moves together with the member, the coordinate transformation matrix has to be updated at each step. Based on the member coordinates  $(x_{n-1}, y_{n-1}, z_{n-1})$  on the  $(n-1)$ -th step, by letting  $(\Delta R_x, \Delta R_y, \Delta R_z)$  be the direction cosine of the increment in the rotation angle occurring between the  $(n-1)$ -th and  $n$ -th steps, the transformation matrix at the  $n$ -th step  $[\mathbf{T}_n]$  becomes Eq. (17). Here  $[\mathbf{T}_0]$  is the initial transformation matrix based on the member's initial position.

$$[\mathbf{T}_n] = [\mathbf{T}_{n-1}][\mathbf{R}_n] = [\mathbf{T}_0] \prod_{i=1}^n [\mathbf{R}_i] \quad (17)$$

$$[\mathbf{R}_n] = \begin{bmatrix} \mathbf{r}_n & \mathbf{0} & \mathbf{0} & \mathbf{0} \\ \mathbf{0} & \mathbf{r}_n & \mathbf{0} & \mathbf{0} \\ \mathbf{0} & \mathbf{0} & \mathbf{r}_n & \mathbf{0} \\ \mathbf{0} & \mathbf{0} & \mathbf{0} & \mathbf{r}_n \end{bmatrix} \quad (18)$$

$$[\mathbf{r}_n] = \begin{bmatrix} 1 + \cos^2 \alpha (\cos \beta - 1) & \sin \alpha \cos \alpha (1 - \cos \beta) & \cos \alpha \sin \beta \\ \sin \alpha \cos \alpha (1 - \cos \beta) & 1 + \sin^2 \alpha (\cos \beta - 1) & \sin \alpha \sin \beta \\ -\cos \alpha \sin \beta & -\sin \alpha \sin \beta & \cos \beta \end{bmatrix} \quad (19a)$$

$$\sin \alpha = \frac{\Delta R_y}{\sqrt{\Delta R_x^2 + \Delta R_y^2}}, \quad \cos \alpha = \frac{\Delta R_x}{\sqrt{\Delta R_x^2 + \Delta R_y^2}}, \quad \sin \beta = \frac{\sqrt{\Delta R_x^2 + \Delta R_y^2}}{\sqrt{\Delta R_x^2 + \Delta R_y^2 + \Delta R_z^2}}, \quad \cos \beta = \frac{\Delta R_z}{\sqrt{\Delta R_x^2 + \Delta R_y^2 + \Delta R_z^2}} \quad (19b)$$



Based on the previous equations, the tangential stiffness equation of the member model in the global coordinate system is given by Eq. (20). The tangential stiffness matrix  $[K]$  of the whole frame is obtained by summing the matrices of all members as shown in Eq. (21).

$$\{\Delta P\} = [T_n][S]\{\Delta p\} = [T_n][S][k]\{\Delta d\} = [T_n][S][k][S]^{-1}[T_n]^{-1}\{\Delta D\} \quad (20)$$

$$[K] = \sum [T_n][S][k][S]^T [T_n]^T \quad (21)$$

## 2.5 Method of Calculation

The stiffness matrix method and the Newmark  $\beta$  method ( $\beta=1/4$ ) are used to analyze time history response during 3-dimension ground motion. The unbalance force arising from the change in elasto-plastic states during each step is eliminated in the next step. Also, at each step an unloading check is performed on each spring of all MS components. If unload occurs at any spring, the stiffness of the spring is substituted with its unloading stiffness and the step is recalculated.

## 3. Parameters and Conditions

### 3.1 Target Frames

The target frames of this study are 4-story 6-6-3, 4-story 6-8-3, 4-story 6-6-1, 6-story 6-6-3, 9-story 6-6-3, 9-story 6-6-1, the elevations and floor plans of the frames are shown in Fig.2 and Fig.3. Each floor is assume to have a long-term load of approximately 7 kN/m<sup>2</sup>, no eccentricity, and follows the rigid floor assumption. The frames are satisfied with the building standard for Japanese seismic design code. Cold-formed square steel columns and wide flange beams are used in the frames, and the column overdesign factor (*COF*) at the all beam-to-column connections is over 1.5.

In addition to number of stories and floor plan, we also consider the *COF* as a parameter. By projecting the full plastic moments of the columns and beams onto the input direction, the *COF* for the input direction is calculated as Eq. (22), where  $\theta$  is the angle between the input direction and the X-axis, the  $M_{bp}$ s the full plastic moments of the beams around the strong-axis (see Fig.4). The  $M_{cpn}$ s are the full plastic moments of the columns around the strong-axis under the long-term axial stress. Since the axial force ratio of square tube columns in most low and mid-level buildings is 0.2 and under, their full plastic moments is nearly independent of the input direction.

$$COF_A = \frac{M_{cpn1} + M_{cpn2}}{(M_{bpX1} + M_{bpX2})\cos\theta + (M_{bpY1} + M_{bpY2})\sin\theta} \quad (20)$$

In the following, we call this *COF* projected to the input direction the appearance column overdesign factor ( $COF_A$ ). The average  $COF_A$ , which refers to the average  $COF_A$  of all connections excluding the connections on the roof and the 1st floor column bases, used was between 1.0 to 1.5.

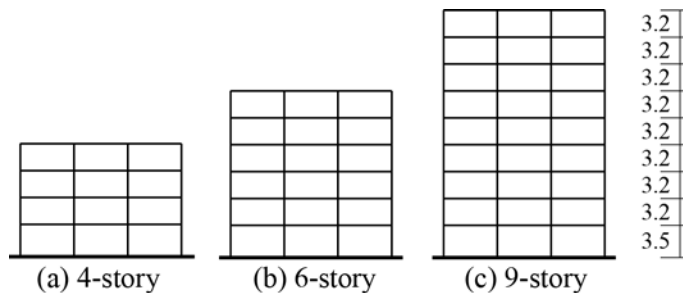


Fig.2 Elevations of frames (unit: meter)

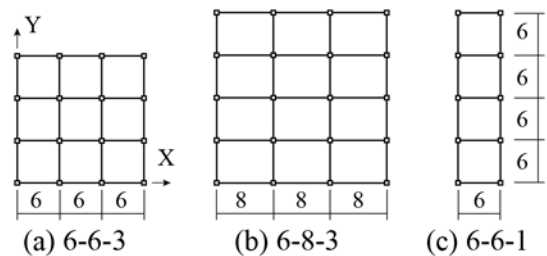
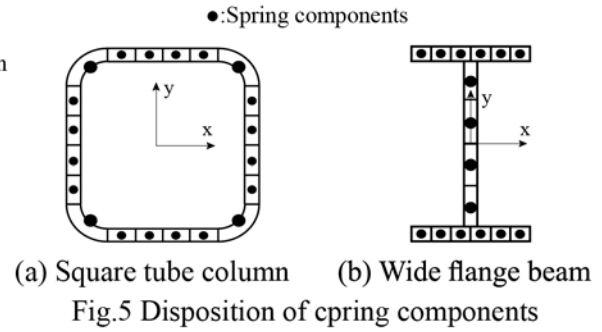
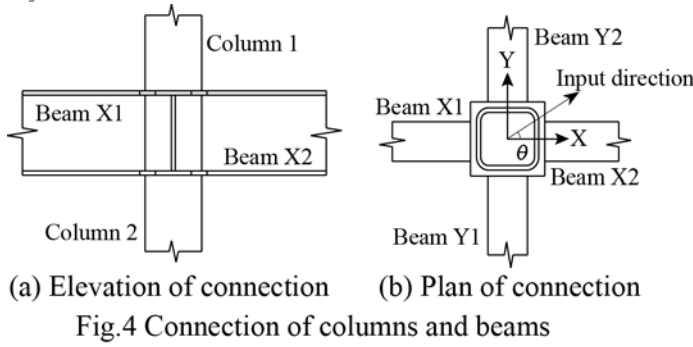


Fig.3 Floor plans (unit: meter)



It is assumed that the higher the horizontal load bearing capacity of the frame, the less plastic deformation response during earthquakes. Hence, we consider frames of similar horizontal load bearing capacity. We adjust the reduction coefficient  $D_s$  of the frames' required horizontal load bearing capacity to 1/3. Note that  $D_s$  is reciprocal of the  $R$  factor [22]. Under the designated average  $COF_A$  and  $D_s$  values for each input direction, the yield stress of the columns and beams are adjusted while keeping the same cross-sections.

### 3.2 Ground Motion Input

For the ground motion input parameter, 0 degrees (X-axis), 45 degrees, 90 degrees (Y-axis) are chosen as input direction, and BCJ L2, El Centro NS, JMA Kobe NS are chosen as ground motion types. Ground motion acceleration was adjusted to ensure the velocity conversion value  $V_{dm}$  of earthquake input energy is almost 1.5 m/s (equivalent to level 2 ground motion in Japanese standard). Here  $V_{dm}$  is given by Eq. (21),  $E_{dm}$  is the maximum earthquake input energy, and  $M$  the mass of the whole frame.

$$V_{dm} = \sqrt{\frac{2E_{dm}}{M}} \quad (21)$$

### 3.3 Conditions on the MS component

- The spring components on the square tube columns and wide flange beams were assigned as in Fig.5.
- To calculate the stiffness of the spring component, the virtual length of the component was taken to be 10% of the actual member length as based on Ref. [23].
- Spring components were assumed to have bilinear restoring force characteristics. The ratio  $k_p$  of the gradients of the strain hardening region to the elastic region is calculated as Eq. (22) according to Ref. [24,25]. Here we consider low to mid-level buildings, with column axial force ratio  $n=0.2$ , beam axial force ratio  $n=0$  to get  $k_p=0.038$  for the columns and  $k_p=0.030$  for beams.

$$k_p = 0.03 + 0.04n \quad (22)$$

### 3.4 Basic Properties of the Frames

Fig.6 shows the sum of the members' energy dissipation in every floor of the original 4-story 6-6-3A frame under El Centro NS. In this paper, we use viscous damping coefficient of 0.02. We see that compared to the average  $COF_A$  of 1.94 at 0°, the average  $COF_A$  at 45° is smaller at 1.36. Hence at 45°, the energy dissipation is small on beam ends but large on the 1st floor column bases. Similar results were observed regardless of the number of stories, floor plan, and type of ground motion.

In order to study the effects of  $COF_A$  regardless of input direction, the yield stress on the columns and beams were adjusted so that the average  $COF_A$  remained at a similar level regardless of input direction in the following studies.

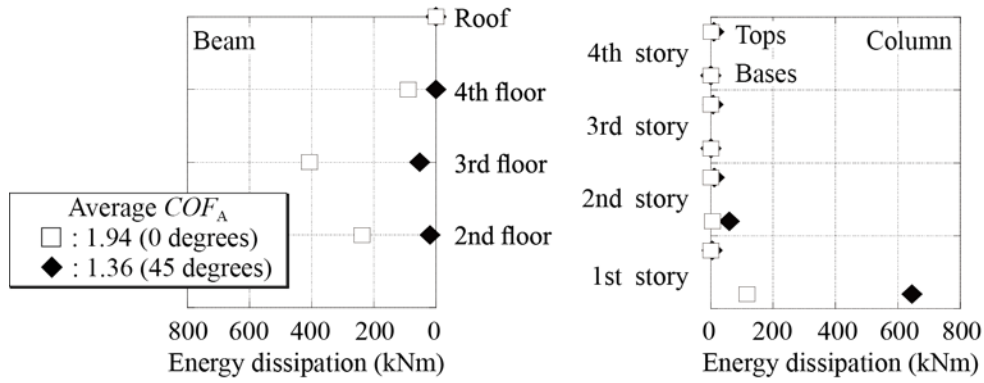


Fig.6 Sum of the members' energy dissipation per floor (original 4-story 6-6-3)

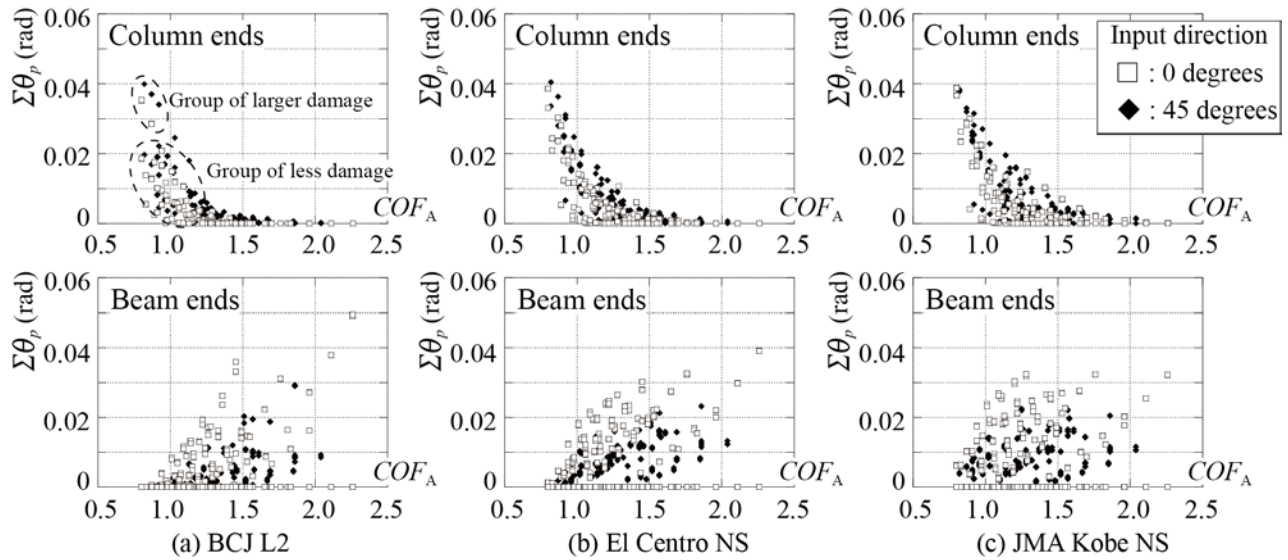


Fig.7  $\Sigma\theta_p$ - $COF_A$  relation of 4-story 6-6-3

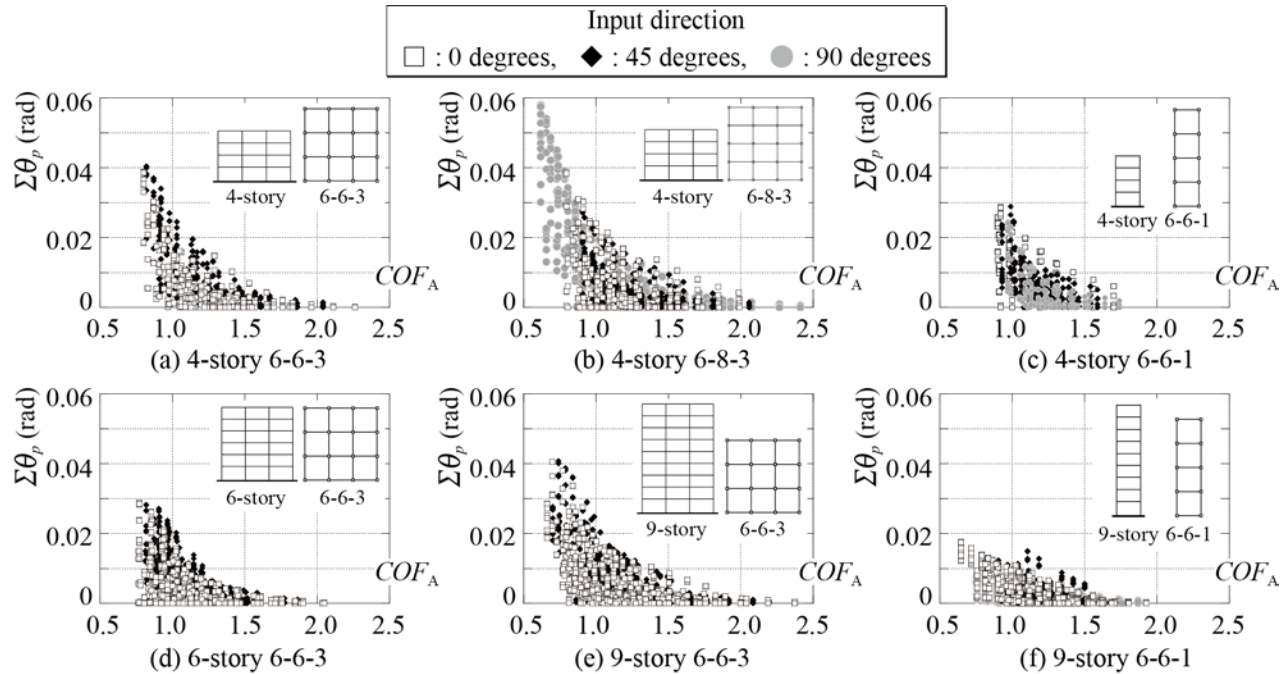


Fig.8 Column  $\Sigma\theta_p$ - $COF_A$  relation



## 4. Results and Discussion

### 4.1 Member Level Damage

In this section we study the effects of appearance column overdesign factor ( $COF_A$ ) on the damage of the members. The results of the time history response analysis on the 4-story 6-6-3 frame with adjusted yield stress are shown in Fig.7, which shows the relation between damage received and  $COF_A$  at each member end. Here, as a measure of damage the cumulative plastic rotational deformation  $\Sigma\theta_p$ , which is the energy dissipation by bending of the member end over its full plastic moment under long-term axial stress, is used.

From Fig.7, we see that the larger the  $COF_A$  the less damage is suffered by the columns, but more damage is suffered by the beams. Comparing Fig.7(a) to Fig.7(b) and (c), the results of BCJ L2 show two different groups of column  $\Sigma\theta_p$  (damage), while El Centro NS and JMA Kobe NS show only 1 each. Also at  $COF_A$  value around 1.0, the results of BCJ L2 show almost no damage to the beams, while El Centro NS and JMA Kobe NS show comparatively significant amounts. This is also because the nature of pulse-like ground motions El Centro NS and JMA Kobe NS which tend to cause damage on the entire frame, while BCJ L2 tends to result in cumulative damage to members with lower full plastic resistance. Similar results were observed regardless of the number of stories, floor plan, and type of ground motion.

### 4.2 Effect of Number of stories and Floor plan

To enable a total collapse mechanism in a frame, it is necessary to reduce the damage to the columns. In the following, we consider only the damage to columns. Fig.8 shows the relation between  $\Sigma\theta_p$  and  $COF_A$  with the results for all ground motion types in one figure for each frame. It shows that the maximum value of column  $\Sigma\theta_p$  and  $COF_A$  follow similar relations regardless of number of stories, floor plan, and input direction of ground motion.

## 5. Required Column Overdesign Factor

### 5.1 Damage Evaluation Index

In this section, we evaluate the relationship between column cumulative plastic rotational deformation  $\Sigma\theta_p$  and appearance column overdesign factor ( $COF_A$ ) obtained from all our cases in order to arrive at the required  $COF_A$ . Fig.9 shows the relationship between the bending moment and the rotation of a member end with deterioration due to local buckling [25].  $\theta_{up}$  is the amount of plastic deformation up until the maximum bending moment in Fig.9. As suggested by [26], we take  $\theta_{up}$  to be the cumulative plastic deformation capacity of square tube column depending on local buckling. Since deterioration behavior is not considered in 3D analysis, the  $\Sigma\theta_p$  is divided by the  $\theta_{up}$  as a index to measure column damage.

In Japan, columns are separated into three ranks, FA (up to width-thickness ratio 33), FB (up to width-thickness ratio 37) and FC (up to width-thickness ratio 48). The frames considered in this paper mainly used FA rank columns. However in this section, since  $\theta_{up}$  changes with the width-thickness ratio, for each rank of column we suggest the  $COF_A$  value needed to contain the damage under a specified value. By assuming that at fixed column resistance the  $\Sigma\theta_p$  remains constant regardless of width-thickness ratio, for each rank we find the value of  $\theta_{up}$  corresponding to its border line width-thickness ratio value. Fig.10 shows the relationship between  $\Sigma\theta_p / \theta_{up}$  and  $COF_A$  for each column rank.

### 5.2 Damage Probability Distribution

In this section, we analyze the probability distribution of the column damage. The main range of consideration 1.0 to 1.5 for the  $COF_A$  is split into 5 intervals. The FA rank column damage probability distribution for the whole  $\Sigma\theta_p / \theta_{up} - COF_A$  relationship as well as each of the 5 intervals is shown in Fig.12. The probability distribution for the whole  $\Sigma\theta_p / \theta_{up} - COF_A$  relationship shown in Fig.11(a) can be approximated using the following probability density function  $f(x)$  as Eq. (23).



$$f(x) = \frac{x^{\alpha-1} e^{-x/\beta}}{\Gamma(\alpha)\beta^\alpha} \tag{23}$$

$$\Gamma(\alpha) = \int_0^\infty t^{\alpha-1} e^{-t} dt \tag{24}$$

Eq. (23) is the gamma distribution with shape parameter  $\alpha$  and rate parameter  $\beta$ . The random variable  $x$  is  $\Sigma\theta_p/\theta_{up}$ ,  $e$  the Napier's constant, and  $\Gamma$  the gamma function. We find the values of  $\alpha$  and  $\beta$  that best approximate our probability distribution. This result is shown by the broken line on Fig. 11(a). From the same figure, we also see that this probability density function Eq. (23) also approximates the probability distribution for each of the intervals. Based on this gamma distribution, the probability that  $x$  is below the mean plus two times the standard deviation is 98.2%. Hence, the required  $COF_A$  can be evaluated with a reliability index of 2.0 by drawing a 98 percentile envelope curve.

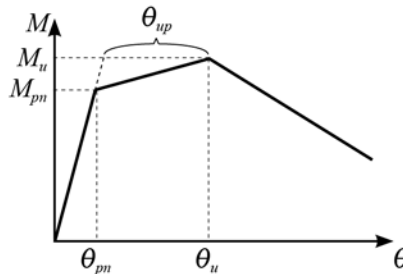


Fig.9  $M-\theta$  relation with deterioration due to local buckling

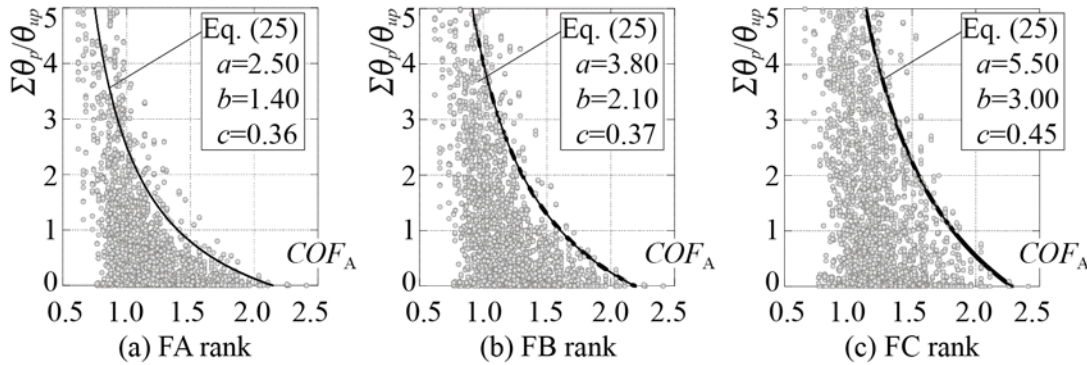


Fig.10  $\Sigma\theta_p/\theta_{up}-COF_A$  relation and envelope curve

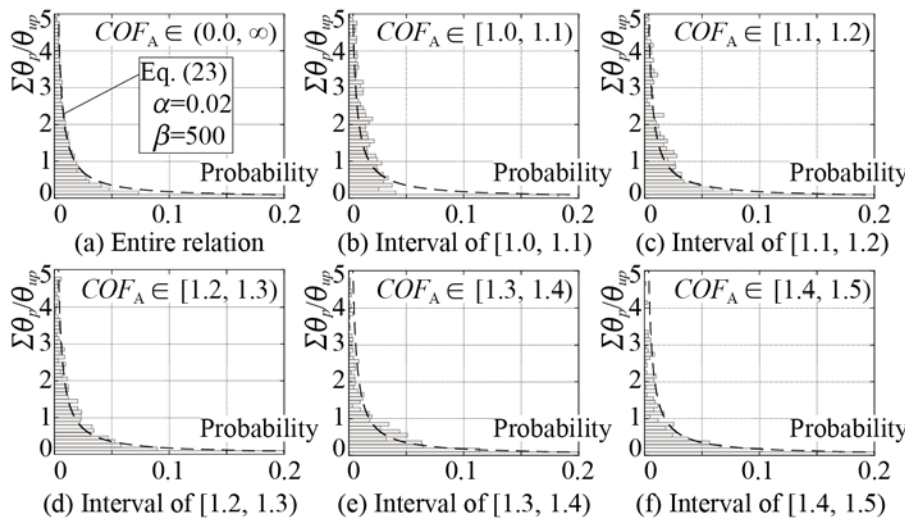


Fig.11 Probability distribution for  $\Sigma\theta_p/\theta_{up}-COF_A$  relation

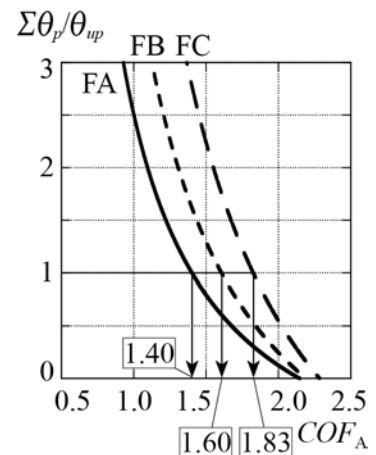


Fig.12 Envelope curve for required  $COF_A$



### 5.3 Envelope Curve of Required $COF_A$

A curve of function as Eq. (25) enveloping at least 98% of the plots in each of the 5 intervals and the entire  $\Sigma\theta_p/\theta_{up}$ - $COF_A$  relation can be drawn in order to find required  $COF_A$  to keep the damage level below the specified value. Envelope curves of required  $COF_A$  for each width-thickness ratio rank are also shown by solid line on Fig.10.

$$COF_A = \frac{a}{\Sigma\theta_p / \theta_{up} + b} + c \quad (25)$$

For example, from Fig.12, which shows the 3 envelope curves on Fig.10 in one figure, the required  $COF_A$  for frames with  $D_s$  value of 1/3, under level 2 ground motion, to keep the cumulative plastic deformation below the performance limit is obtained as 1.40 for square tube columns of FA rank width-thickness ratio, and 1.60 for FB rank, 1.83 for FC rank, respectively.

## 6. Conclusion

This paper described the damage of each member by 3D analysis of steel moment frames with square tube columns, and presented seismic demand for the appearance column overdesign factor ( $COF_A$ ) to keep the damage of columns below the specified limit of plastic deformation. The major parameters are  $COF_A$  of beam-column connections, number of stories, the planar shape of frames, input direction of ground motions. The major findings obtained from this study are as follows.

- i) With the similar horizontal load bearing capacity of the frames, The profile of maximum value of column cumulative plastic deformation  $\Sigma\theta_p$  to  $COF_A$  are nearly identical regardless of number of stories, floor plan, and input direction of ground motion.
- ii) As an index to evaluate the damage of columns, the plastic deformation capacity  $\theta_{up}$  of square tube columns depending on local buckling is adopted for different rank of width-thickness ratio, and the damage level of columns is defined as the value obtained by dividing  $\Sigma\theta_p$  by  $\theta_{up}$ . From the relationship between  $\Sigma\theta_p/\theta_{up}$  and  $COF_A$ , the required  $COF_A$  to keep the damage level below the specified value is proposed for frames with  $D_s$  value of 1/3 under level 2 ground motion.

Further more, geometrical nonlinearity and the behaviors of connection panel and composite beam are not considered in this paper. These are the future tasks.

## 7. References

- [1] Masayoshi Nakashima, Charles W. Roeder and Yoshiomi Maruoka (2008): Steel moment frames for earthquakes in United States and Japan, *Journal of Structural Engineering*, **126**(8), 861-868
- [2] AISC (2010): ANSI/AISC 341-10. *Seismic Provisions for Structural Steel Buildings*, American Institute of Steel Construction, Inc., Chicago, IL.
- [3] The Building Center of Japan (2013): *The Building Standard Law of Japan*. Tokyo: The Building Center of Japan
- [4] Koji Ogawa (1983): On the optimum elastic limit strength distribution of structural members in steel frames, Part 2 numerical examples. *Transactions of the Architectural Institute of Japan*, **328**, 18-25 (in Japanese)
- [5] Takayuki Teramoto and Haruyuki Kitamura (1986): The inelastic response of steel frames subjected to strong ground motion, effect of the column/girder ratio and vertical distribution of strength. *Transactions of the Architectural Institute of Japan*, **363**, 57-66 (in Japanese)
- [6] Kazuo Inoue, Koji Ogawa, Motohide Tada and Hidekazu Ynagihara (1994): Earthquake response of member plastic deformation of rigid frames with RHS columns, Part2 analytical results. *Summaries of Technical Papers of Annual Meeting Architectural Institute of Japan*, Structures II 1994, 1303-1304 (in Japanese)



- [7] Takashi Hasegawa and Hiroyuki Yamanouchi (1994): Required deformation capacity of steel structural members based on damage distribution in steel frames under strong earthquake ground motions. *Journal of Structural and Construction Engineering*, **460**, 169-177 (in Japanese)
- [8] Takashi Hasegawa, Akio Kadono, Hisaya Kamura, Koji Fukuda, Tomohide Someya and Yoshihiro Hamazaki (1996): Earthquake response analysis of rigid frames with rbs columns allowing for deformation of joint panels. *Journal of Architecture and Building Science*, **2**, 43-48 (in Japanese)
- [9] H. Lee (1996): Revised rule for concepts of strong-column weak-girder design. *Journal of Structural Engineering*, **122** (4), 359-364
- [10] Sang-hoon Oh, Satoshi Yamada and Hiroshi Akiyama (1998): Damage distribution rule of weak beam type multi-story steel frames influenced by strength and stiffness ratios of beam and column. *Journal of Structural and Construction Engineering*, **506**, 171-177 (in Japanese)
- [11] Sutat Leelataviwat, Subhash C. Goel and Boz'idar Stojadinovic' (1999): Toward Performance Based Seismic Design of Structures, *Earthquake Spectra*, **15**(3), 435-461
- [12] Masayoshi Nakashima and Shinichi Sawaizumi (1999): Effect of column-to-beam strength ratio on earthquake responses of steel moment frames, Part 1 column-to-beam strength ratio required for ensuring beam-hinging responses. *Steel Construction Engineering*, **6**(23), 117-132 (in Japanese)
- [13] Shinichi Sawaizumi and Masayoshi Nakashima (1999): Effect of column-to-beam strength ratio on earthquake responses of steel moment frames, Part 2 response characteristics of frames involving column yielding. *Steel Construction Engineering*, **6**(23), 133-148 (in Japanese)
- [14] Rita Bento and Mário Lopes (2000): Evaluation of the need for weak beam-strong column design in dual frame-wall structures, 12th World Conference on Earthquake Engineering, Auckland, New Zealand
- [15] K. Khandelwal, S. El-Tawil, S. Kunnath and H. Lew (2008): Macromodel-based simulation of progressive collapse: steel frame structures. *Journal of Structural Engineering*, **134** (7), 1070-1078
- [16] Se Woon Choi and Hyo Seon Park (2012): Multi-objective seismic design method for ensuring beam-hinging mechanism in steel frames, *Journal of Constructional Steel Research*, **74**, 17-25
- [17] Akira Wada and Keiichi Hirose (1989): Elasto-plastic dynamic behaviors of the building frames subjected to bi-directional earthquake motion. *Journal of Structural and Construction Engineering*, **399**, 37-47 (in Japanese)
- [18] Ryoma Kimura and Koji Ogawa (2007): Effect of column-to-beam strength ratio on maximum story drift angle response of steel frames under horizontal bi-directional ground motions. *Steel Construction Engineering*, **14**(55), 111-121 (in Japanese)
- [19] Yoshinori Sakai and Koji Ogawa (2010): Pertinent column-to-beam strength ratio of steel frames subjectd to horizontal bidirectional ground motions. *Steel Construction Engineering*, **17**(67), 53-64 (in Japanese)
- [20] Yuji Koetaka and Manabu Kanada (2011): Effects of input earthquake direction and hysteresis characteristics on seismic response of steel structures. *Steel Construction Engineering*, **18**(69), 17-32 (in Japanese)
- [21] Takashi Hasegawa and Akio Hori (2012): Three dimensional earthquake response analysis of existing non-conformed steel frames using STKR columns against 45-degree directional input earthquake motions. *Journal of Structural Engineering*, **58B**, 413-421 (in Japanese)
- [22] Chia-Ming Uang (1991): Comparison of seismic force reduction factors used in U.S.A. and Japan. *Earthquake Engineering & Structural Dynamics*, **20**, 389-397
- [23] Koichi Takanashi and Ken-ichi Ohi (1911): Multi-spring joint model for inelastic behavior of steel members with local buckling. *Stability and Ductility of Steel Structures under Cyclic Loading*, **3**, 215-224
- [24] Ben Kato, Hiroshi Akiyama and Yooichi Obi (1977): Deformation characteristics of h-shaped steel members influenced by local buckling. *Transactions of the Architectural Institute of Japan*, **257**, 49-58 (in Japanese)
- [25] Ben Kato, Hiroshi Akiyama and Susumu Kitazawa (1978): Deformation characteristics of box-shaped steel members influenced by local buckling. *Transactions of the Architectural Institute of Japan*, **268**, 71-76 (in Japanese)
- [26] Ben Kato and Hiroshi Akiyama (1968): The ultimate strength of the steel beam-column part 4. *Transactions of the Architectural Institute of Japan*, **151**, 15-20 (in Japanese)